Geomechanics and Engineering, Vol. 1, No. 1 (2009) 35-52
DOI: http://dx.doi.org/10.12989/gae.2009.1.1.035

Shear strength characteristics of a compacted soil under infiltration conditions

H. Rahardjo†, I. Meilani and E. C. Leong

School of Civil and Environmental Engineering, Nanyang Technological University, Singapore

R. B. Rezaur

Department of Civil Engineering, Universiti Teknologi Petronas, 31750 Tronoh, Perak, Malaysia

(Received December 12, 2008, Accepted March 5, 2009)

Abstract. A significantly thick zone of steep slopes is commonly encountered above groundwater table and the soils within this zone are unsaturated with negative pore-water pressures (i.e., matric suction). Matric suction contributes significantly to the shear strength of soil and to the factor of safety of unsaturated slopes. However, infiltration during rainfall increases the pore-water pressure in soil resulting in a decrease in the matric suction and the shear strength of the soil. As a result, rainfall infiltration may eventually trigger a slope failure. Therefore, understanding of shear strength characteristics of saturated and unsaturated soils under shearing-infiltration (SI) conditions have direct implications in assessment of slope stability under rainfall conditions. This paper presents results from a series of consolidated drained (CD) and shearing-infiltration (SI) tests. Results show that the failure envelope obtained from the shearing-infiltration tests is independent of the infiltration rate. Failure envelopes obtained from CD and SI tests appear to be similar. For practical purposes the shear strength parameters from the CD tests can be used in stability analyses of slopes under rainfall conditions. The SI tests might be performed to obtain more conservative shear strength parameters and to study the pore-water pressure changes during infiltration.

Keywords: shear strength; triaxial test; consolidated drained test; shearing-infiltration tests; pore-water pressure.

1. Introduction

Matric suction contributes significantly to the shear strength of soil (Lim *et al.* 1996, Han 1997, Melinda 1998, Wong *et al.* 2001, Anderson and Sitar 1995, Ng and Chiu 2003, Melinda *et al.* 2004). Variation in matric suction influences the shear strength of a soil in zones above the groundwater table. High matric suction in a slope gives an additional factor of safety to the slope. However, infiltration during rainfall increases the pore-water pressure in the soil resulting in a decrease in the matric suction and the shear strength of the soil (Brand *et al.* 1984, Lim *et al.* 1996, Rahardjo *et al.* 2001, Wei *et al.* 1991, Melinda *et al.* 2004). This process may eventually trigger a landslide.

† Professor, Corresponding author, E-mail: chrahardjo@ntu.edu.sg

Yoshida *et al*. (1991) noted that reduction in strength due to infiltration of rainfall is the major cause for triggering slope failures. Many researchers in civil engineering attempted to simulate the failure mechanism of soils due to the infiltration of rainfall using laboratory models. However, limitation due to heterogeneity of soils and difficulties associated with adopting an appropriate testing method has hampered the study of the mechanism of rainfall-induced slope failures.

Brand (1981) proposed that rainfall-induced slope failures should be simulated in a shear strength test under a constant total stress and increasing the pore-water pressure. Some researchers have investigated the shear strength of soils under shearing-infiltration conditions (Sasitharan *et al*. 1993, Anderson and Sitar 1995, Anderson and Riemer 1995, Brenner *et al*. 1995, Han 1997, Melinda 1998, Wong *et al*. 2001, Ng and Chiu 2001, 2003, Melinda *et al.* 2004). However, the characteristics of the pore-water pressure changes have not been thoroughly studied due to the limitations of pore-water pressure measuring devices for unsaturated soil testing. In addition, the characteristics of shear strength, particularly the characteristics of the failure envelope under infiltration conditions in unsaturated soils have not been fully understood. Therefore, pore-water pressure measurement in unsaturated soil testing and shear strength characteristics of unsaturated soils under infiltration conditions warrant a careful investigation.

The objective of this study is therefore to study; (i) the shear strength characteristics of saturated and unsaturated soils under shearing-infiltration conditions; and (ii) the pore-water pressure characteristics of saturated and unsaturated soils during infiltration and at pre-failure conditions.

2. Methodology

The methodology for the study comprised three steps: (i) modifying or assembling two triaxial apparatuses for consolidated drained (CD) and shearing infiltration (SI) tests; (iii) specimen preparation; and (iv) designing the experimental procedure for CD and SI tests.

2.1 Modified triaxial apparatus for CD and SI tests

CD tests were performed in a modified triaxial apparatus similar to the modified triaxial apparatus described by Fredlund and Rahardjo (1993). The modified triaxial apparatus for the CD tests consisted of a triaxial compression cell, compression machine, digital pressure and volume controller (DPVC), linear variable differential transformer (LVDT), auto-volume change indicator (AVCI), diffused-air volume indicator (DAVI), data acquisition unit and a personal computer. Prior to test, all the transducers, load cell, LVDT, AVCI were calibrated.

SI test were performed by using another modified triaxial apparatus designed and constructed by Wong *et al*. (2001). The modified triaxial apparatus consisted of a large triaxial cell, three mini suction probes for pore-water pressure measurements, a force actuator for shearing and maintaining a constant axial force on the specimen and an additional DVPC for water infiltration. The three mini suction probes were installed at the ¾ (i.e., "top"), ½ (i.e., "middle") and ¼ (i.e., "bottom") heights of a specimen from its base and at 120 degrees apart in the lateral circumferential direction and was used to measure the pore-water pressures along the height of a specimen. Detailed installation procedure for the mini suction probes is described in Meilani *et al*. (2002). All transducers were connected to a data logger and readings are obtained using a personal computer. The force actuator and DPVC were also controlled by the personal computer. A computer control program, Triax 4.0

Table 1 Properties of soil (kaolin) used in the study

Properties	Value
Specific gravity, G_s	2.65
Bulk density, $\rho_{d\ max}$ (Mg/m^3)	1.35
Optimum water content, w_{opt} (%)	22
Liquid limit, LL	51
Plastic limit, PL	36
Plasticity index, PI	15
Sand content	0
Silt silt (%)	15
Clay content (%)	85
USCS*	MH
Swelling potential (%)	1.89
Swelling pressure (kPa)	27
Collapse potential (%)	0.06
Saturated permeability, k_{sat} (m/s)	6.40×10^{-8}
Permeability at pore-water pressure 100 kPa (m/s)	2.01×10^{-8}
Permeability at pore-water pressure 200 kPa (m/s)	4.44×10^{-9}

*USCS = Unified Soil Classification System (ASTM, 1997)

(Toll 1999), was used for data acquisition.

2.2 Specimen Preparation

To ensure homogeneity of the soil, specimens were prepared identically. Table 1 shows the properties of the coarse kaolin from Kaolin Malaysia SDN BHD (Malaysia) used in the study. The kaolin was statically compacted to a maximum dry density of 1.35 Mg/m^3 at 22% optimum water content. A fixed displacement rate of 1 mm/min was applied by a compression machine to obtain a specimen with a diameter of 50 mm and a height of 100 mm.

2.3 Consolidated Drained (CD) and Shearing Infiltration (SI) test program

A summary of combination of confining pressure and constant matric suction used in consolidated drained (CD) and shearing-infiltration (SI) tests on saturated and unsaturated specimens is shown in Table 2. Within each series of tests, all combinations of confining pressure and constant matric suction (within parenthesis, see Table 2) were studied.

Four CD tests at effective confining pressures of 25, 50, 100, and 200 kPa were performed on saturated specimens. Twenty CD tests with a combination of 4 levels of net confining pressure (25, 50 100, and 200 kPa) and 5 levels of constant matric suction (15, 30, 50, 100, and 200 kPa) were performed on unsaturated specimens (Table 2).

Three SI tests at effective confining pressures of 50, 100, and 200 kPa and at a constant low infiltration rate of 0.04 mm^3/s were performed on saturated specimens. Nine SI tests with a combination of 3 levels of net confining pressure (25, 100, and 200 kPa) and 3 levels of constant matric suction (50, 100, and 200 kPa) under a constant low infiltration rate of 0.04 mm^3/s was performed on

Table 2 Summary of combination of confining pressure and constant matric suctions used in consolidated drained (CD) and shearing infiltration (SI) tests on saturated and unsaturated specimens

Test Type	Specimen condition	Effective confining pressure, $(\sigma_3 - u_w)$ (kPa)	Net confining pressure, $(\sigma_3 - u_a)$ (kPa)	Constant matric suction, $(u_a - u_w)$ (kPa)	Infiltration rate (mm^3/s)	No of Tests
CD Test	Saturated	$\begin{bmatrix} 25 \\ 50 \\ 100 \\ 200 \end{bmatrix}$	N/A	N/A	N/A	4
CD Test	Unsaturated	N/A	$\begin{bmatrix} 25 \\ 50 \\ 100 \\ 200 \end{bmatrix}$	$\begin{bmatrix} 15 \\ 30 \\ 50 \\ 100 \\ 200 \end{bmatrix}$	N/A	20
SI Test	Saturated	$\begin{bmatrix} 50 \\ 100 \\ 200 \end{bmatrix}$	N/A	N/A	Low rate (0.04 mm^3/s)	3
SI Test	Unsaturated	N/A	$\begin{bmatrix} 50 \\ 100 \\ 200 \end{bmatrix}$	$\begin{bmatrix} 50 \\ 100 \\ 200 \end{bmatrix}$	Low rate (0.04 mm^3/s)	9
SI Test	Unsaturated	N/A	25	100	High rate (0.25 mm^3/s)	1
SI Test	Unsaturated	N/A	200	200	High rate (0.25 mm^3/s)	1

Note: Within each type of test, all combinations of variable levels (within parenthesis) were studied.

unsaturated specimens (Table 2). Two additional SI tests were performed on unsaturated specimens under a constant high infiltration rate of 0.25 mm^3/s with net confining pressures of 25 and 200 kPa and corresponding to constant matric suction of 100 and 200 kPa, respectively (Table 2).

Specimens and test results were identified using notations as CDS 25-200 (LR). The first two alphabets identifies the test type (CD for consolidated drained test or SI for shearing infiltration test), the third alphabet identifies specimen condition (S for saturated condition or U for unsaturated condition), the first set of numbers in the specimen notation represents the effective confining pressure for saturated specimens or the applied net confining pressure for unsaturated specimens. The second set of numbers after the separator sign represents the applied matric suction and the last two alphabets within parenthesis represents infiltration rate (LR for low infiltration rate or HR for high infiltration rate). Thus a test identified by CDS 25-200 (LR) represents a consolidated drained test on saturated specimen using a low infiltration rate and at an applied effective confining pressure of 25 kPa and a constant matric suction of 200 kPa. Similarly, a test identified by SIU 25-200 (HR) represents a shearing-infiltration test on an unsaturated specimen using a high infiltration rate and at an applied net confining pressure of 25 kPa and a constant matric suction of 200 kPa.

The CD test consisted of three stages for the saturated specimens (i.e., saturation, consolidation, and shearing stages) and four stages for the unsaturated specimens (i.e., saturation, consolidation, matric suction equalization, and shearing stages). During saturation stage, the specimen was saturated by applying cell pressure and back pressure (Head 1986). Pore pressure parameter B of 0.95 was used to confirm full saturation. After saturation, the specimen was consolidated to the desired effective confining pressure. Subsequently, the shearing stage was carried out on saturated specimens when there was no more excess pore-water pressure. During the matric suction equalization stage on unsaturated specimens, the matric suction in the specimen was controlled using the axis-translation technique (Hilf 1956). Pore-air pressure was controlled from the top cap through a coarse porous stone. Pore-water pressure was controlled from the base through a 5-bar high air-entry ceramic disk. Matric suction equalization was considered to be accomplished when there were no more changes in water volume. The saturated and unsaturated specimens were sheared at a constant cell pressure with the same strain rate of 0.0008 mm/min until failure occurred. The optimum strain rate of 0.0008 mm/min was used during the shearing stage in order to reduce the testing duration in triaxial test on an unsaturated specimen. In addition, the strain rate was sufficient to allow pore-water pressure dissipation in saturated and unsaturated specimens. Shearing was carried out at a constant cell pressure on saturated and unsaturated specimens. The stress path followed by the specimen in a CD test under constant matric suction is illustrated in Fig. 1. Point F (in Fig. 1) represents the initial condition of the specimen. The stress path moved from point F to point O during the saturation stage. The specimen was then consolidated under an applied net confining pressure as shown in Fig. 1 from point O to A. In the matric suction equalization stage, the stress path moved along path AB. Loading of the specimen started at point B until failure occurred at point D.

SI tests on unsaturated specimens consisted of saturation, consolidation, matric suction equalization, shearing, and infiltration stages. The matric suction equalization stage was not conducted in the SI test on saturated specimens. Saturation, consolidation and matric suction equalization stages in the SI tests were the same as the corresponding procedures used in the CD tests. During the infiltration stage, water was injected from the base at a constant rate of 0.04 mm^3/s while the top drainage was kept closed. The deviator stress was maintained constant and therefore, there was no shear strain applied to the specimen. The rate of water injection allowed the transient pore-water pressure development to be observed during the shearing-infiltration test. The rate or water injection used in this study was similar to those used by Han (1997), Melinda (1998) and Wong *et al.* (2001). Prior to the infiltration stage, the specimen was sheared to 85-90% of peak shear stress as obtained from the CD test. The range of 85 to 90% of peak shear stress was chosen as the shear stress in steep slopes under field condition can be as high as 85 to 90% of peak shear stress.

The stress path for each stage in the SI tests is illustrated in Fig. 1. The stress path moves along path FOAB during the saturation stage, consolidation stage and matric suction equalization stage. Shearing started at point B and stopped at point C which was 85-90% of peak shear stress as obtained from the CD test. During the infiltration stage, the deviator stress was maintained by the force actuator while water was injected from the base using DPVC. The stress path during the infiltration stage followed path CE until the specimen failed under infiltration at point E.

When a decline in the deviator stress or an excessive increase in the strain rate commenced during a shearing-infiltration test, the specimen was considered to have failed. This failure criteria for specimen was based on previous shearing-infiltration test studies on residual soils from Bukit Timah Granite in Singapore (Han 1997, Melinda 1998, Wong *et al.* 2001) and on soils from Briones Hills

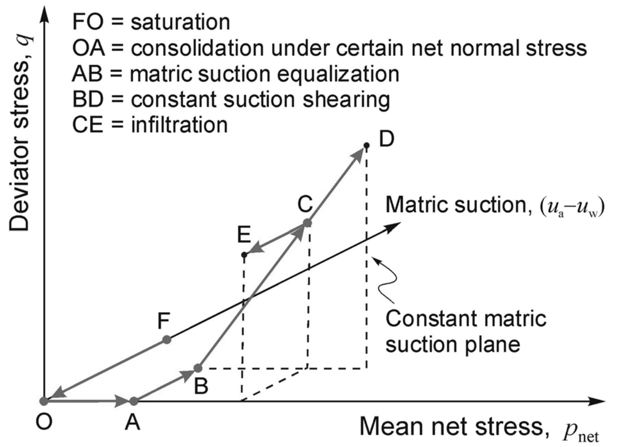

Fig. 1 Schematic representation of stress paths of specimens at triaxial testing

field site (Anderson and Sitar 1995) which used the start of a decline in the deviator stress or the start of an excessive increase in the strain rate as the failure criteria for a shearing-infiltration test.

3. Results and discussion

3.1 Failure envelopes from the CD tests

Fig. 2 shows the stress paths from the CD tests under a constant matric suction of 0 kPa, 25 kPa, 50 kPa, 100 kPa and 200 kPa. The inflection points along the x-axis in Fig. 2 were derived from the inflection points along the Mohr-coulomb failure envelope. The mean effective stress p', mean net stress p_{net}, and deviator stress q, are defined as

$$p' = \text{mean effective stress} = \left(\frac{\sigma_1 + \sigma_3}{2}\right) - u_w$$

$$p_{net} = \text{mean net stress} = \left(\frac{\sigma_1 + \sigma_3}{2}\right) - u_a$$

$$q = \text{deviator stress} = \left(\frac{\sigma_1 - \sigma_3}{2}\right)$$

where, σ_1 and σ_3 are the major and minor principal stresses.

Table 3 summarizes the intercept (d), of the failure envelope on the q-axis, the inflection point along the x-axis, the angle of failure envelope (ψ'_1) with respect to p_{net} before the inflection point, and the angle of failure envelope (ψ'_2) with respect to p_{net} axis after the inflection point, that were obtained from the stress paths from the CD tests (Fig. 2). As the matric suction increased the intercept (d) of the failure envelope on the q-axis increased from 14 kPa to 48 kPa. The angle ψ'_1 is consistent between 33° to 34° (with the exception of ψ'_1 = 30° at matric suction of 50 kPa) while ψ'_2 increased from 25° to 27°. The failure envelope on the q versus (u_a-u_w) plane obtained from the CD test on unsaturated specimens is shown in Fig. 3. The variation of angle ψ^b which indicates the

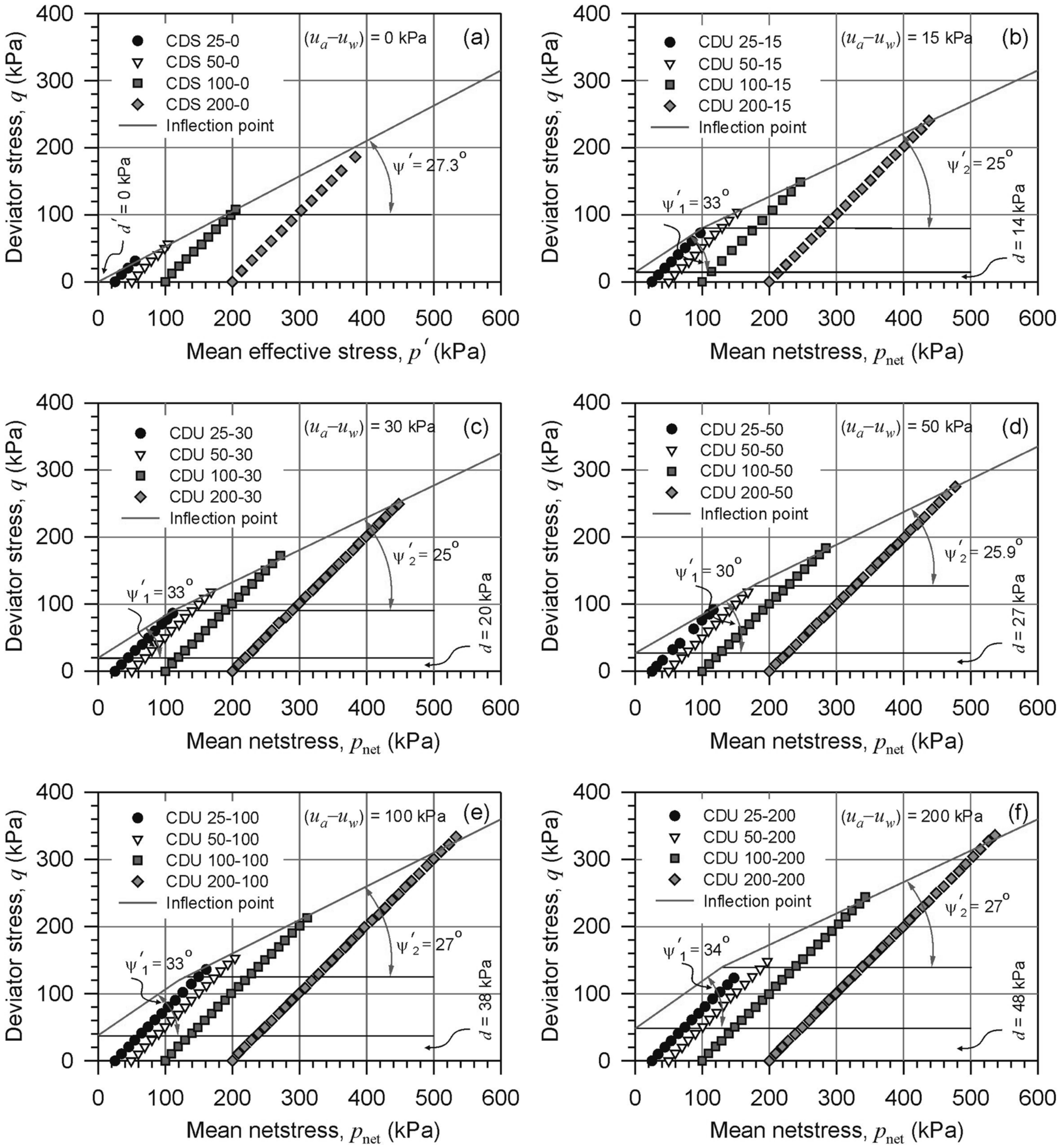

Fig. 2 Stress paths from consolidated drained tests of saturated and unsaturated specimens under various net confining pressures and a constant matric suction of (a) 0 kPa; (b) 15 kPa; (c) 30kPa; (d) 50 kPa; (e) 100 kPa; and (f) 200 kPa

rate of change in d with respect to changes in matric suction at zero net stress are shown in Fig. 3. Fig. 3 shows that the angle ψ^b decreased from 43° to 5.7° as the matric suction increased from 0 to 200 kPa.

Table 3 Summary of shear strength parameters obtained from failure envelopes shown in Fig. 2

No.	Matric suction, $(u_a - u_w)$ (kPa)	d, (kPa)	Inflection point along the x-axis (kPa)	ψ_1' (°)	ψ_2' (°)
1	15	14	100	33	25
2	30	20	106	33	25
3	50	27	184	30	25.9
4	100	38	131	33	27
5	200	48	128	34	27

Note: d = intercept of the failure envelope on the q-axis (kPa); ψ_1' = angle of failure envelope with respect to p_{net} -axis before the inflection point (°); ψ_2' = angle of failure envelope with respect to p_{net} -axis after the inflection point (°)

3.2 Failure envelopes from SI test

To show the behavior of specimens during shearing-infiltration test one of the shearing-infiltration tests results from unsaturated specimen SIU 25-200 (LR) is presented in Fig. 4. Test SIU 25-200 (LR) was conducted in a single stage loading under 25 kPa net confining pressure and 200 kPa matric suction. The specimen was first saturated and then consolidated under 25 kPa effective confining pressure and 200 kPa initial matric suction. During the shearing stage the specimen was sheared until the deviator stress reached 85% of the peak deviator stress. The deviator stress was then maintained constant at this value until the end of the shearing-infiltration test. Water was then injected from the base at a low infiltration rate of 0.04 mm^3/s until the specimen failed during the infiltration stage.

In expressing the test results, total volumetric strain (ε_v), was defined as the ratio between the total volume change and the initial total volume of the specimen. Water volumetric strain (ε_w), was defined as the ratio between the water volume change and the initial total volume of the specimen. The sign convention used in presenting the triaxial test results was that; a positive total volumetric

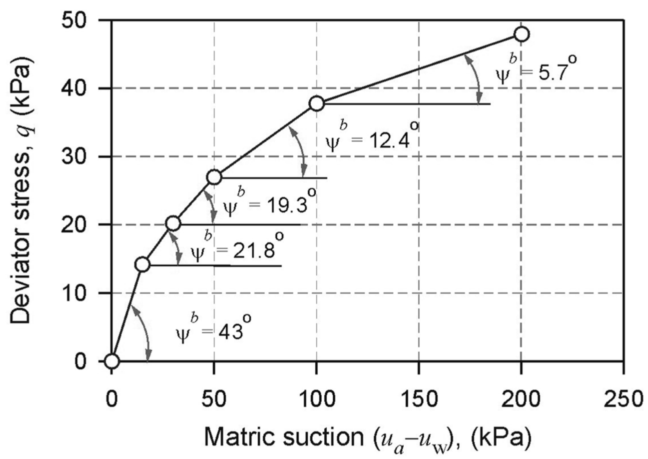

Fig. 3 Failure envelope on the q versus $(u_a - u_w)$ plane indicating the rate of change (ψ^b) in d with respect to changes in matric suction

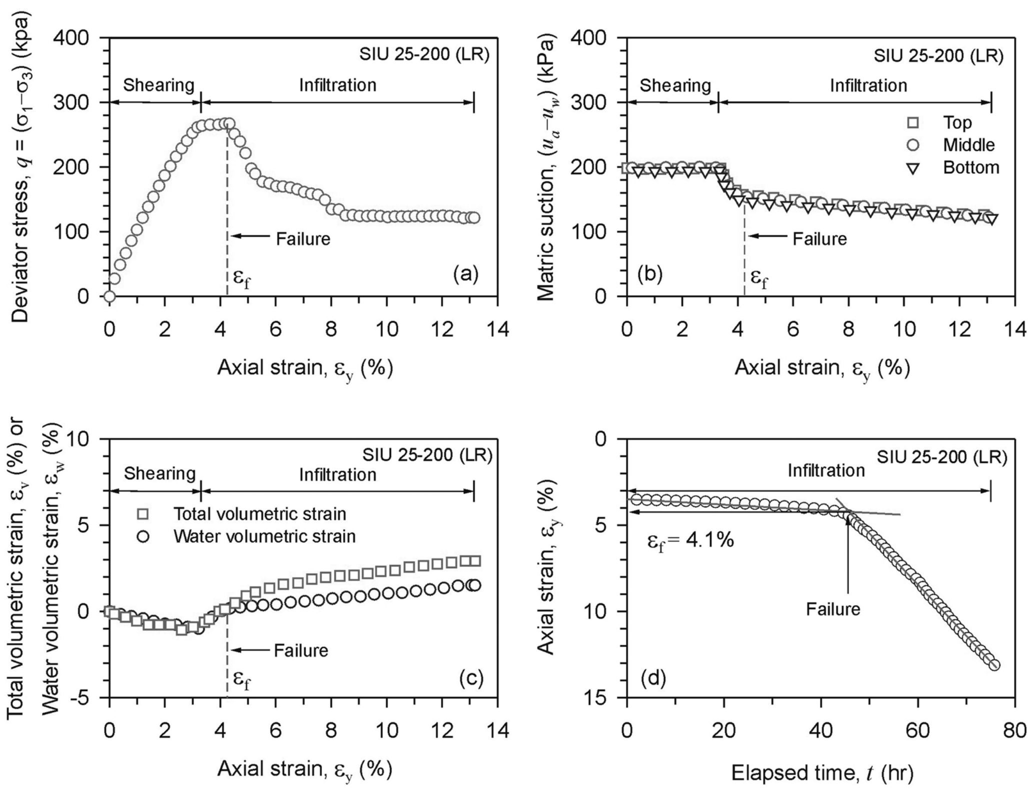

Fig. 4 Behaviour of a saturated specimen (SIU 25-200 (LR)) during shearing-infiltration at a low infiltration rate; (a) variation in deviator stress ($\sigma_1 - \sigma_3$) in response to changes in axial strain (ε_y); (b) variation in matric suction ($u_a - u_w$) in response to changes in axial strain (ε_y); (c) variation in volumetric strain (ε_v) and water volume strain (ε_w) in response to changes in axial strain (ε_y); (d) determination of failure point

strain indicates the dilation of the specimen while a negative total volumetric strain shows compression. A positive water volumetric strain indicates that water infiltrates into the specimen and a negative water volumetric strain indicates that the pore-water drains out from the specimen. In addition, a positive axial strain demonstrates that the specimen is compressing and a negative axial strain demonstrates swelling of the specimen in the vertical direction.

Fig. 4a shows variation in deviator stress ($\sigma_1-\sigma_3$), in response to changes in axial strain (ε_y), throughout the shearing and infiltration stages of SI test on specimen SIU 25-200 (LR). The specimen was sheared to 85% of its peak deviator stress (i.e., 268 kPa) and maintained at 268 kPa during the infiltration stage. As can be seen in Fig. 4a, the deviator stress could not be maintained by the computer control program after failure occurred. The deviator stress dropped gradually after failure due to the shearing-infiltration on specimen SIU 25-200 (LR).

Fig. 4b shows variation in matric suction in response to changes in axial strain (ε_y), throughout the shearing and infiltration stages of SI test on specimen SIU 25-200 (LR). The readings from the mini suction probes along the height of the specimen demonstrate that the matric suction remained constant during the shearing process (Fig. 4b). The pore-air and pore-water pressure were under drained conditions during the shearing stage. During the infiltration stage, the pore-air pressure was

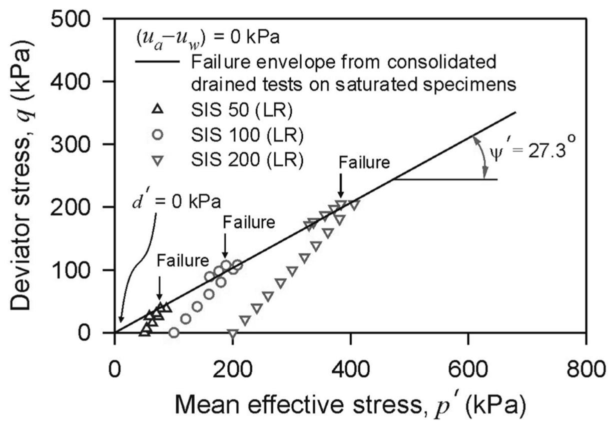

Fig. 5 Stress paths from shearing-infiltration test of saturated specimens

under drained while the pore-water pressure was found to increase thus the matric suction decreased. The average value of matric suctions at failure from the top (i.e., 155.7 kPa), middle (i.e., 152.4 kPa) and bottom (i.e., 148.7 kPa) probes was 152.3 kPa.

Fig. 4c illustrates the total volumetric strain and water volumetric strain in specimen SIU 25-200 (LR) during the shearing and infiltration stages of the SI test. During the shearing stage, the specimen was subjected to compression because water drained out from the specimen. On the other hand, a positive volumetric strain (i.e., dilation) was induced during the infiltration stage when water was injected from the bottom of the specimen.

Fig. 4d shows the changes in axial strain (ε_y), with elapsed time (t), during the infiltration stage of specimen SIU 25-200 (LR). The axial strain increased sharply after failure. In order to find the axial strain at failure (ε_f), two tangent lines were drawn on the axial strain versus elapsed time curve and were extended to intercept each other. The intersection point indicated that the axial strain at failure (ε_f) was 4.1%. Figs. 4a to 4c indicates that at $\varepsilon_f = 4.1\%$ the corresponding deviator stress, matric suction, total volumetric strain and water volumetric strain at failure are 266 kPa, 152 kPa, 0.31% and 0.13%, respectively.

Fig. 5 shows the stress paths from the SI test on saturated specimens SIS 50 (LR), SIS 100 (LR) and SIS 200 (LR). The intercept (d') of the failure envelope on the q-axis from SI tests on saturated specimens was 0 kPa and the angle of failure envelope (ψ') with respect the p'-axis was found to be 27.3°. For comparison the failure envelope from CD tests on saturated specimens are also plotted in Fig. 5. As expected, the failure envelope from the SI tests on saturated specimen seems to be same as the failure envelope from the CD tests on saturated specimens. The saturated specimens for SI tests were under drained condition during the shearing stage but were under undrained condition during the infiltration stage. As the pore-water pressure increased due to injection of water, the stress path moved to the left and eventually coincided with the failure envelope from the CD tests (Fig. 5).

Fig. 6 shows the comparison between the failure envelopes from the CD tests on unsaturated specimens and the stress paths from nine SI tests on unsaturated specimens at the same p_{net} value. The stress paths from two SI tests (i.e., SIU 25-50 (LR) and SIU 100-100 (LR)) are not presented here because these specimens had not reached failure due to equipment breakdown. The SI tests on unsaturated specimens demonstrate that the failure envelope obtained from the shearing-infiltration

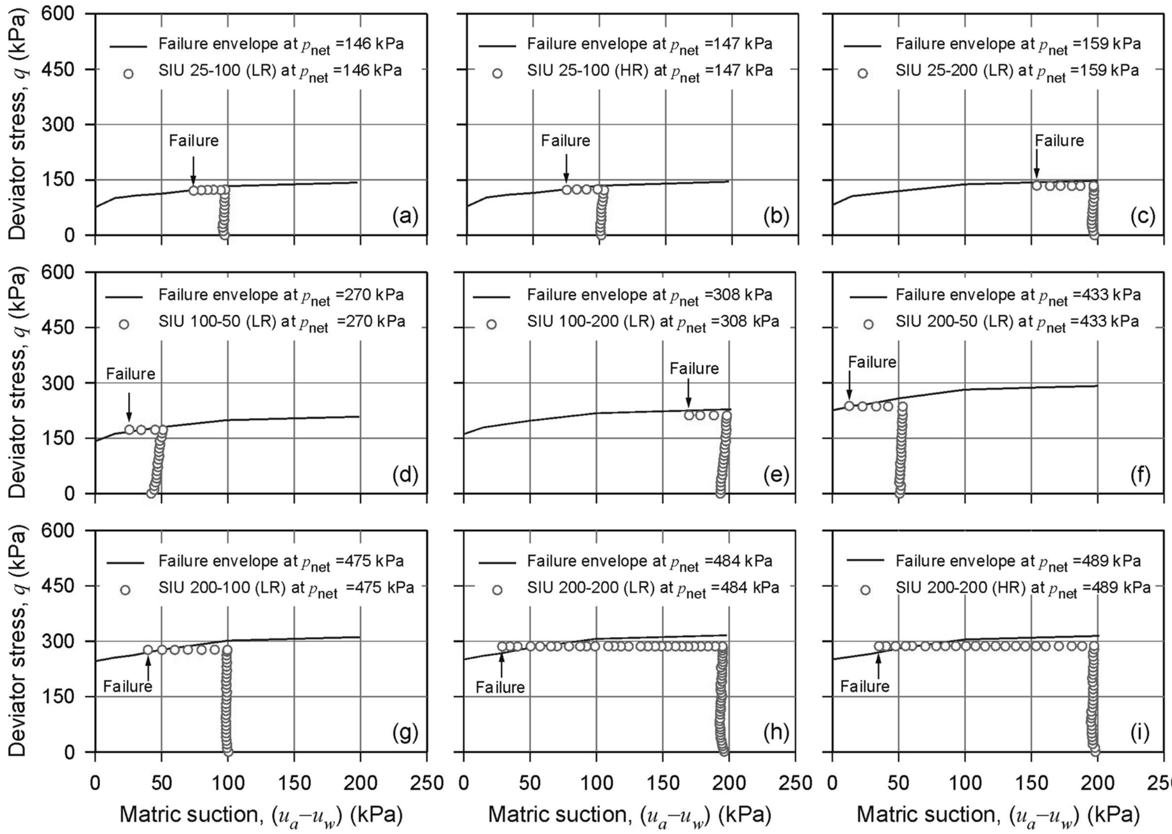

Fig. 6 Comparison between the failure envelopes from CD tests on unsaturated specimens and stress paths from SI test on unsaturated specimen at the same p_{net} value

tests is unique regardless of the infiltration rate and valid at least for the range of data investigated (Meilani *et al.*, 2005). Fig. 6 also suggests that, unsaturated specimens with the same net confining pressure and initial matric suction when subjected to shearing-infiltration tests under low or high infiltration rates showed failure at the same matric suction. For instance, unsaturated specimens SIU 25-100 (LR) and SIU 25-100 (HR) subjected to low and high infiltration rates, respectively during the SI test failed at the same matric suction of 75 kPa (see Figs. 6a and 6b). Similarly, specimens SIU 200-200 (LR) and SIU 200-200 (HR) subjected to low and high infiltration rates, respectively failed at nearly the same matric suction of 30 kPa and 35 kPa, respectively (see Figs. 6h and 6i). Of course, the time required to fail the specimen will depend on soil type and stress state (mean net stress and matric suction) of the specimen.

Fig. 7 shows a comparison between the failure envelope with respect to mean effective stress (i.e., q versus p') and mean net stress (i.e., q versus p_{net}) obtained from the SI and CD tests on matric suction planes of 0 kPa, 15 kPa, 30 kPa, 50 kPa, 100 kPa and 200 kPa. In general, there is no significant difference between ψ' values obtained from the SI and CD tests at various p_{net} values on the constant matric suction plane of 0 kPa, 15 kPa, 100 kPa and 200 kPa (Figs. 7a, 7b, 7e and 7f). However, there is a difference of 2.5 times to 3 times between ψ' values obtained from the SI and CD tests at various p_{net} values on the constant matric suction plane of 30 kPa and 50 kPa (Figs. 7c,

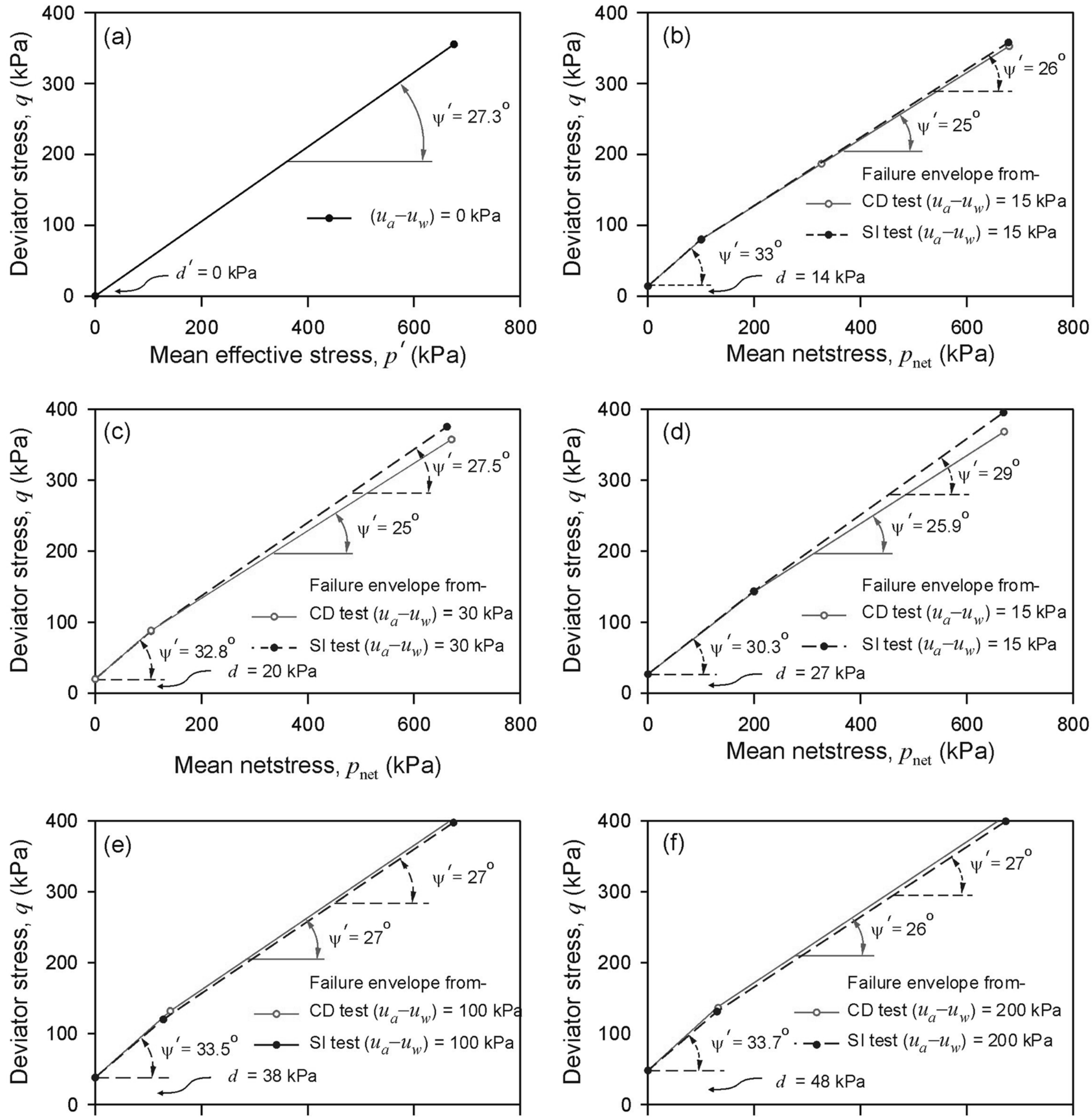

Fig. 7 Comparison between failure envelopes from CD and SI tests under different matric suctions: (a) 0 kPa; (b) 15 kPa; (c) 30 kPa; (d) 50 kPa; (e) 100 kPa; (f) 200 kPa

7d). The failure envelope (i.e., q versus p_{net}) for unsaturated specimens (i.e., $(u_a - u_w) \neq 0$ kPa) shows non-linearity at around a p_{net} value of 150 kPa. At p_{net} values less than 150 kPa, ψ' is around 30-33^o and at p_{net} values greater than 150 kPa, ψ' is around 25-27^o.

Fig. 8 shows the comparisons between the failure envelope with respect to matric suction (i.e., q versus $(u_a - u_w)$) obtained from the SI and CD tests at a constant p' and p_{net} planes of 0 kPa, 150 kPa, 300 kPa and 450 kPa. The failure envelope (i.e., q versus $(u_a - u_w)$) from the SI tests is the

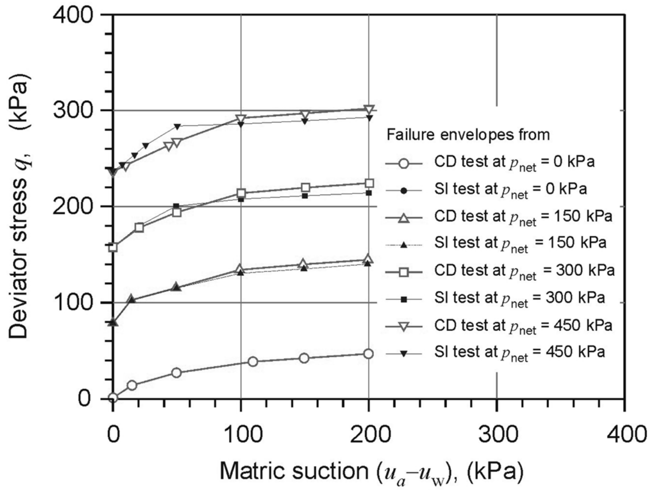

Fig. 8 Comparison between failure envelopes from the CD and SI tests at different mean net stress, p_{net}

same as the failure envelope (i.e., q versus $(u_a - u_w)$) from the CD tests for p_{net} value of 0 kPa at all matric suction values and for p_{net} value of 150 kPa at matric suctions less than 80 kPa. These characteristics can also be observed from the SI tests results from unsaturated specimens SIU 25-100 (LR), SIU 25-100 (HR) and SIU 200-50 (LR) shown in Fig. 6 (Figs. 6a, 6b and 6f).

It is observed that generally the failure envelope from the SI tests is similar to the failure envelope from the CD tests. However, slight difference was noticed at p_{net} values from 150 to 450 kPa depending on the matric suction. The failure envelope from the SI tests is higher than the failure envelope from the CD tests at matric suctions from 0 to 80 kPa while the failure envelope from the SI tests is lower than the failure envelope from the CD tests at matric suction higher than 80 kPa. Nevertheless, considering the number of tests performed, the natural variability of the samples prepared and limitation in the laboratory testing equipment, the minor differences can be

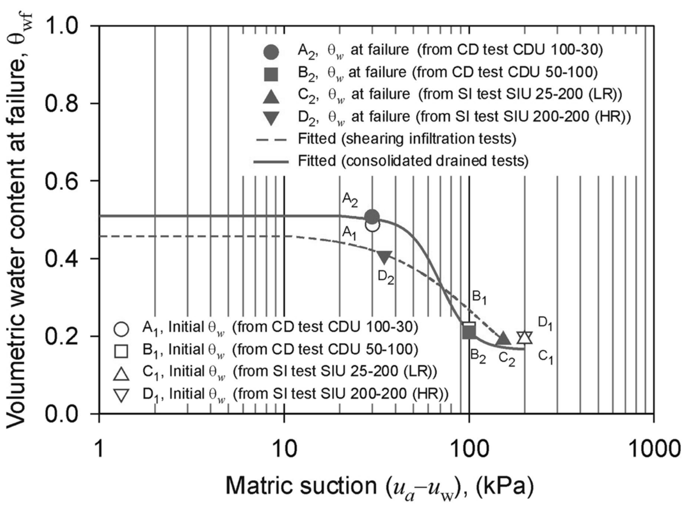

Fig. 9 The volumetric water content from CD tests and SI tests

considered negligible or in other words, the failure envelope from the SI tests is similar to the failure envelope from the CD tests.

In order to determine the type of shear strength tests required for the stability assessment of a slope under rainfall infiltration conditions, this study postulated that the shear strength from the consolidated drained tests gives more conservative results than the shearing-infiltration tests. In addition, the shearing-infiltration test may not be necessary due to its tedious test procedure unless the pore-water pressures during infiltration conditions need to be studied. However, shearing-infiltration tests might be performed to obtain more realistic shear strength parameters under infiltration conditions for specimens at p_{net} values higher than 150 kPa (i.e., specimens at depths around 8 meters) with a matric suction higher than 80 kPa.

The characteristics of the failure envelopes from the CD and SI tests on unsaturated soils can be related to their volumetric water contents. The relationship between the volumetric water content at failure (θ_{wf}), and the matric suction ($u_a - u_w$), for the SI and CD tests are illustrated in Fig. 9. A comparison between Fig. 9 and Fig. 8 shows that between 0 kPa and 80 kPa matric suction range the volumetric water content curve from the SI tests is lower than that from the CD tests (Fig. 9) whereas, the failure envelopes from the SI tests are higher than that from the CD tests (Fig. 8). On the other hand, a reverse trend is observed at matric suctions greater than 80 kPa. At matric suction range greater than 80 kPa the volumetric water content curve from the SI tests is higher than that from the CD tests (Fig. 9) whereas the failure envelopes from the SI tests are lower than that from the CD tests (Fig. 8). It can therefore be deduced that a low volumetric water content gives a higher shear strength to the soils or in other words a higher volumetric water content produces a lower shear strength of the soils.

The reverse trend in the volumetric water contents can be explained in terms of the difference in stress paths for each stage in the CD and SI tests. Point C1 to C2 and point D1 to D2 show the volumetric water content during shearing-infiltration stage in the SI tests (Fig. 9). The volumetric

Table 4 Residual deviator stress $(\sigma_1 - \sigma_3)_r$, failure mode, degree of saturation at failure S_f, and matric suction at failure $(u_a - u_w)_f$, from shearing infiltration tests on unsaturated specimens

Test	Deviator stress before infiltration, $(\sigma_1-\sigma_3)_i$, (kPa)	Residual deviator stress, $(\sigma_1-\sigma_3)_r$, (kPa)	Ratio, $\frac{(\sigma_1-\sigma_3)_r}{(\sigma_1-\sigma_3)_i}$ (%)	Failure mode	Degree of saturation at failure, S_f (%)	Matric suction at failure, $(u_a-u_w)_f$ (kPa)
SIU 25-50 (LR)	188			N/A		
SIU 25-100 (LR)	245	129	53	Brittle	70.84	74.60
SIU 25-100 (HR)	245	159	65	Brittle	59.00	74.40
SIU 25-200 (LR)	268	123	46	Brittle	39.39	152.30
SIU 100-50 (LR)	339	304	89	Ductile	≈100.00	26.00
SIU 100-100 (LR)	298			N/A		
SIU 100-200 (LR)	432	272	63	Brittle	40.67	164.60
SIU 200-50 (LR)	467	409	88	Ductile	≈100.00	12.60
SIU 200-100 (LR)	550	488	89	Ductile	93.70	39.50
SIU 200-200 (LR)	578	575	100	Ductile	95.40	29.40
SIU 200-200 (HR)	578	504	87	Ductile	91.97	34.80

Table 5 Matric suction at failure from shearing infiltration tests on unsaturated specimens

Test	Net confining pressure, $(\sigma - u_a)$ (kPa)	Matric suction before infiltration $(u_a - u_w)_i$ (kPa)	Matric suction at failure $(u_a - u_w)_f$ (kPa)	Reduction of matric suction $1 - \frac{(u_a - u_w)_f}{(u_a - u_w)_i}$ (%)
SIU 100-50 (LR)	100	50	26.0	49.33
SIU 200-50 (LR)	200	50	12.6	76.30
SIU 25-100 (LR)	25	100	75.3	24.39
SIU 25-100 (HR)	25	100	74.4	27.84
SIU 200-100 (LR)	200	100	39.5	60.38
SIU 25-200 (LR)	25	200	152.3	22.86
SIU 100-200 (LR)	100	200	164.6	16.15
SIU 200-200 (LR)	200	200	29.4	85.03
SIU 200-200 (HR)	200	200	34.8	82.27

water content increased from point A1 to A2 during shearing in the CD tests under a constant matric suction less than 80 kPa. In contrast, the volumetric water content decreased from point B1 to B2 during shearing in the CD tests under a constant matric suction higher than 80 kPa. As a result, the volumetric water content at failure from the CD tests are higher between 0 to 80 kPa matric suction range and lower at matric suctions greater than 80 kPa. Therefore, the volumetric water content curve from the SI tests is lower than the volumetric water content curve from the CD tests at matric suctions less than 80 kPa (Fig. 9) and higher at matric suction greater than 80 kPa (Fig. 9).

3.3 Characteristics of shear strength from the SI tests

The characteristics of shear strength from the SI tests were found to depend on the degree of saturation or the value of matric suction at failure. The failure mode observed in the SI tests on the saturated specimens SIS 50 (LR), SIS 100 (LR) and SIS 200 (LR) was ductile. Table 4 shows the failure mode, degree of saturation at failure (S_f), and matric suction at failure, $(u_a - u_w)_f$, from the SI tests on unsaturated specimens. The failure mode was ductile for specimens which failed at a degree of saturation higher than 90% or at a matric suction in the range of 0 kPa to 50 kPa. On the other hand, the failure mode was brittle for specimens which failed at a degree of saturation lower than 90% or at a matric suction higher than 50 kPa. The 90% degree of saturation at failure therefore, can be used as a limit to determine the failure mode. Ductile failures occurred at $[(\sigma_1 - \sigma_3)_r/(\sigma_1 - \sigma_3)_i]$ ratio higher than 80% and brittle failures occurred at $[(\sigma_1 - \sigma_3)_r/(\sigma_1 - \sigma_3)_i]$ ratio lower than 80%. It is also important to note that specimens that exhibited brittle failure, the residual deviator stress after failure ranged between 46-65% of the deviator stress before the infiltration stage commenced.

3.4 Characteristics of matric suction from the SI tests

During the SI tests since the specimens were sheared under a drained condition there was no change in matric suction condition throughout the shearing stage. During the infiltration stage water was injected from the base until failure occurred. As water infiltrated into the specimen, the matric suction decreased during the infiltration stage. Table 5 shows the average matric suction at failure $(u_a - u_w)_f$, (average of mini suction probe reading at specimen top, middle and bottom) and the percentage of reduction in matric suction at failure $(u_a - u_w)_f$, from the matric suction before infiltration $(u_a - u_w)_i$. Results presented in Table 5 suggests that under the same initial matric suction a larger reduction in matric suction occurred in specimens subjected to a larger net confining pressures. For example, specimens SIU 100-50 (LR) and SIU 200-50 (LR) had a net confining pressure of 100 kPa and 200 kPa, respectively. The percentages of reduction in matric suction from the matric suction before infiltration for these specimens were 49.33% and 76.30%, respectively.

The net confining pressure in soils at shallow depths of a slope is generally low, therefore, a small reduction in matric suction due to infiltration can cause failure for soils at shallow depths. On the other hand, the net confining pressure in soils at greater depths is high and a large reduction in matric suction during rain infiltration is required to cause failure in soils at greater depths. Therefore, it is easier for soils at shallow depths than soils at greater depths to fail during a rainfall as commonly observed in shallow slip surfaces of rainfall-induced slope failures. However, cracks, which allow water from rainfalls to penetrate to greater depths may also cause a large reduction in matric suction and trigger failure in soils at greater depths.

4. Conclusions

The SI tests on unsaturated specimens demonstrated that the failure envelope obtained from the SI tests is unique in the sense that they are independent of the infiltration rate. Unsaturated specimens subjected to low infiltration rate (SIU 25-100 (LR)) and high infiltration rate (SIU 25-100 (HR)) during SI tests showed failure at the same matric suction of 75 kPa. Other SI tests on unsaturated specimens with low (SIU 200-200 (LR)) and high (SIU 200-200 (HR)) infiltration rates but different net confining pressure and matric suction also failed at almost the same matric suctions of 30 kPa and 35 kPa, respectively.

The failure envelope from the SI tests is similar to the failure envelope from the CD tests. For practical purposes the shear strength parameters from CD tests can be used in stability analyses of slopes under rainfall conditions. The SI test is recommended for obtaining more conservative shear strength parameters and studying the pore-water pressure during infiltration at p_{net} values higher than 150 kPa (i.e., soils at depths around 8 meters) with a matric suction higher than 80 kPa.

Ductile failure can be assumed to occur at $[(\sigma_1 - \sigma_3)_r/(\sigma_1 - \sigma_3)_i]$ ratio higher than 80%. As a result, it can be implied that ductile failure occurred at a degree of saturation at failure (S_f) higher than 90%. These findings were derived for the coarse kaolin; therefore further study needs to be carried out for other soil types.

The percentage of reduction in matric suction during infiltration is higher for a higher mean net stress. A large percentage of reduction in matric suction is required to cause failure in soils at a high mean net stress, p_{net} value. On the other hand, a small percentage of reduction in matric suction can trigger failure in soils at a low p_{net} value. The effect of matric suction and p_{net} values on the failure envelopes obtained from the CD and SI tests can be explained using the volumetric water content at failure (θ_{wf}). A lower volumetric water content gives a higher shear strength or conversely, a higher volumetric water content produces a lower shear strength of the soils.

Acknowledgements

This study was funded by research grants (NSTB: 17/6/16 and No: RG7/99) from the National Science and Technology Board, Singapore and the Nanyang Technological University, Singapore. The second author acknowledges the scholarship received from the Nanyang Technological University, Singapore.

References

Anderson, S.A. and Riemer, M.F. (1995), "Collapse of saturated soil due to reduction in confinement", *J. Geotech. Eng.*, *ASCE*, **121**(2), 216-220.
Anderson, S.A. and Sitar, N. (1995), "Analysis of rainfall-induced debris flows", *J. Geotech. Eng.*, *ASCE*, **21**(7), 544-552.
ASTM. (1997), "Annual Book of ASTM Standards", American Society for Testing and Materials (ASTM), Philadelphia, PA. Vol. 04.08-04.09.
Brand, E.W. (1981), "Some thoughts on rain-induced slope failures", *Proceedings of the 10th International Conference on Soil Mechanics and Foundation Engineering*, Stockholm, **3**, 373-376.
Brand, E.W., Premchitt, J. and Philipson, H.B. (1984), "Relationship between rainfall and landslides in Hong Kong", *Proceeding of the 4th International Symposium on Landslides*, Toronto, Canada, 377-384.
Brenner, R.P., Tan, H.K. and Brand, E.W. (1985), "Field stress path simulation of slope failure", *Proceedings of the 11th International Conference of Soil Mechanics and Foundation Engineering*, San Francisco, **2**, 991-996.
Fredlund, D.G. and Rahardjo, H. (1993), *Soil Mechanics for Unsaturated Soils*, John Wiley and Sons Inc., New York.
Han, K.K. (1997), "Effect of hysteresis, infiltration and tensile stress on the strength of an unsaturated soil", Ph.D. Thesis, Nanyang Technological University, Singapore.
Head, K.H. (1986), *Manual of Soil Laboratory Testing*, John Wiley and Sons, Inc., **3**, 942-945.
Hilf, J.W. (1956), "An investigation of pore-water pressure in compacted cohesive soils", Ph.D. Thesis, Tech. Memo. No. 654, U.S. Dep. of the Interior, Bureau of Reclamation, Design and Construction Div., Denver, C.O.
Lim, T.T., Rahardjo, H., Chang, M.F. and Fredlund, D.G. (1996), "Effect of rainfall on matric suctions in a residual soil slope", *Can. Geotech. J.*, **33**, 618-628.
Meilani, I., Rahardjo, H. and Leong, E.C. (2005), "Pore-water Pressure and water volume change of an unsaturated soil under infiltration conditions", *Can. Geotech. J.*, **42**(6), 1509-1531.
Meilani, I., Rahardjo, H., Leong, E.C. and Fredlund, D.G. (2002), "Mini suction probe for matric suction measurement", *Can. Geotech. J.*, **39**(6), 1427-1432.
Melinda, F. (1998), "Shear strength of a compacted residual soil from unsaturated direct shear tests", M. Engg. Thesis, Nanyang Technological University, Singapore.
Melinda, F., Rahardjo, H., Han, K.K. and Leong, E.C. (2004), "Shear strength of compacted soil under infiltration condition", *J. Geotech. Geoenviron. Eng.*, **130**(8), 807-817.
Ng, C.W.W. and Chiu, A.C.F. (2001), "Behavior of a loosely compacted unsaturated volcanic soil", *J. Geotech. Geoenviron. Eng.*, *ASCE*, **127**(12), 1027-1036.
Ng, C.W.W. and Chiu, A.C.F. (2003), "Laboratory study of loose saturated and unsaturated decomposed granitic soil", *J. Geotech. Geoenviron. Eng.*, *ASCE*, **129**(6), 550-559.
Rahardjo, H., Li, X.W., Toll, D.G. and Leong, E.C. (2001), "The effect of antecedent rainfall on slope stability", *Geotech. Geol. Eng.*, **19**, 371-399.
Sasitharan, S., Robertson, P.K., Sego, D.C. and Morgenstern, N.R. (1993), "Collapse behaviour of sand", *Can. Geotech. J.*, **30**(4), 569-577.
Toll, D.G. (1999), *A data acquisition and control system for geotechnical testing*, In: B. Kumar and B.H.V. Topping (eds.) Developments in Civil and Structural Engineering, Edinburgh Computing, Civil-Comp Press, 237-242.

Wei, J., Heng, Y.S., Chow, W.C. and Chong, M.K. (1991), "Landslides at Bukit Batok Sports Complex", *Proceeding of the 9th Asia Conference on Soil Mechanics and Foundation Engineering*. Bangkok, Thailand, Balkema, Rotterdam, 445-448.

Wong, J.C., Rahardjo, H., Toll. D.G. and Leong, E.C. (2001), "Modified triaxial apparatus for shearing-infiltration test", *Geotech. Test. J.*, **24**(4), 370-380.

Yoshida, Y., Kuwano, J. and Kuwano, R. (1991), "Rain-induced slope failures caused by reduction in soil strength", *Soils Found.*, **31**(4), 187-193.

CC